



# Detached Eddy Simulation of the Flow Noise Generation of Cylinders with Porous Cover

Thomas F. Geyer\*, Sparsh Sharma†

*Brandenburg University of Technology Cottbus - Senftenberg, 03046 Cottbus, Germany*

Ennes Sarradj‡

*Technische Universität Berlin, 10587 Berlin, Germany*

The use of porous materials is a known method for the reduction of cylinder vortex shedding noise. In a previous experimental wind tunnel study, the noise reducing effect of a modification of circular cylinders with open-porous materials was shown. The cylinder models consisted of a solid core cylinder with porous covers with different material parameters. In order to obtain insight into the flow through the porous materials, the noise generation by such porous-covered cylinders is investigated numerically using Detached-Eddy Simulations. This was done for three different porous material covers as well as for a non-porous reference cylinder at three Reynolds numbers in the critical flow regime. Unlike the observations from the experiments, the numerical results show that fluid enters the porous materials and vortex shedding also takes place at the inner core cylinder, leading to an additional tone in the acoustic far field spectrum. In addition, the porous covers were found to have no effect on the directivity of the aeolian tone and to lead to a notable reduction of the aerodynamic drag.

## I. Introduction

The noise generated by a cylinder in a flow is a main source of aeroacoustic noise. It contains both broadband noise and tonal noise, due to the regular shedding of vortices, and can be found at components of the landing gear of airplanes, at the pantograph of trains, at antennas and other protruding parts of vehicles.

One possible method for the reduction of aeroacoustic noise from cylinders is the use of flow permeable materials, which has been the subject of various studies in the past. This includes both experimental investigations [1–7] and numerical work [8–11]. In addition to a reduction of noise, such materials also affect the flow around the cylinder and, subsequently, the aerodynamic drag [12–20]. In a previous experimental study by the authors [5], the noise reducing effects of a large number of different flow permeable cylinder covers were shown. Thereby, the cylinder models consisted of a non-porous core cylinder on which hollow cylinder disks made of porous material were threaded. The study featured a large variety of porous materials, characterized by their air flow resistivity. However, many of the materials had rather high air flow resistivities, as materials with very low air flow resistivities and hence a high permeability tend to be very soft and therefore hard to manufacture into the desired shapes. Thus, several questions remained unanswered, including a hypothesis regarding the cause of the noise reduction.

The focus of the present study is to provide insight into the flow phenomena involved, especially the flow through the porous materials, by performing a numerical simulation. In addition, it is of interest if it is possible to reproduce the existing experimental results with the chosen numerical setup, especially with the simplifying description of the porous materials.

\*Research Assistant, Technical Acoustics Group, Brandenburg University of Technology Cottbus - Senftenberg, Germany.

†Research Assistant, Technical Acoustics Group, Brandenburg University of Technology Cottbus - Senftenberg, Germany.

‡Professor, Institute of Fluid Mechanics and Engineering Acoustics, Technical University Berlin, Germany.

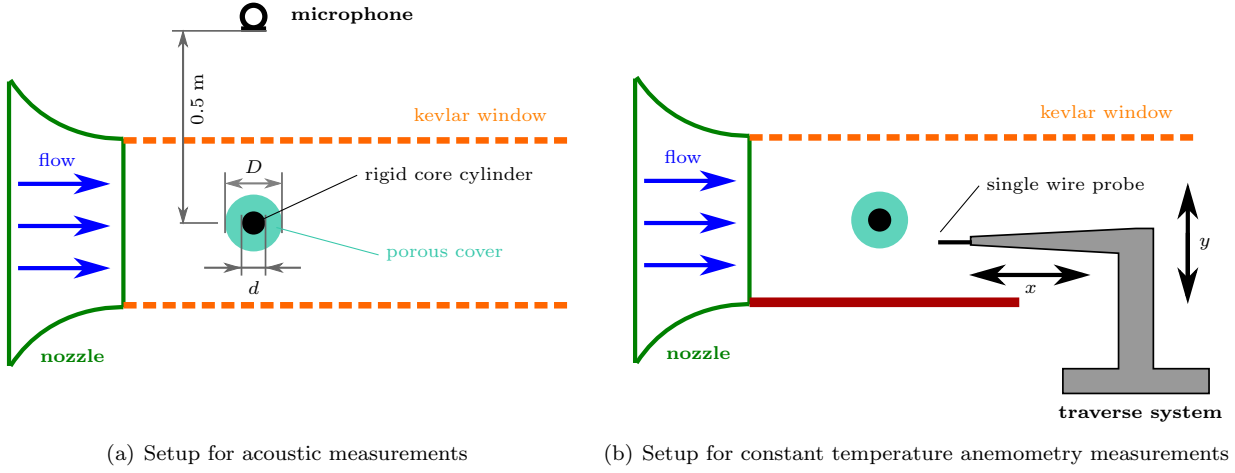


Figure 1. Experimental setup in the aeroacoustic open-jet wind tunnel (top view)

Table 1. Porous covered cylinders used in the experiments

Name	Material	Description	Air Flow Resistivity ( $\text{Pa s/m}^2$ )
Porous 1	Packing foam	Polyurethane foam	4,100
Porous 2	Basotect	Melamine resin foam	9,800
Porous 3	Damtec Estra	Rubber granulate	12,900
Porous 4	Commetall Rubber Mat	Rubber granulate	53,200
Porous 5	Damtec USM	Rubber granulate	86,100
Porous 6	ArmaFoam Sound	Elastomer foam	112,100
Reference	PVC	non-porous	$\infty$

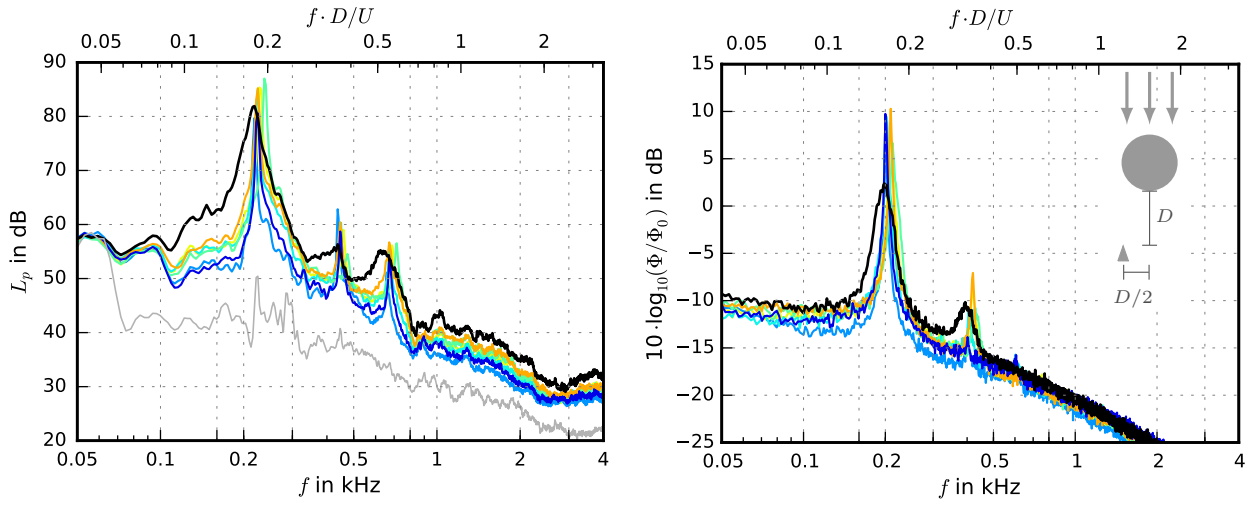
## II. Experimental Investigation

### II.A. Setup

The experiments took place in the small aeroacoustic wind tunnel at BTU Cottbus - Senftenberg [21], using a rectangular nozzle with an exit diameter of  $0.23 \text{ m} \times 0.28 \text{ m}$  and a test section with side windows covered with tensioned Kevlar. In order to avoid sound reflections, the test section is surrounded by a cabin with absorbing side walls. The acoustic measurements were performed using a one fourth inch free-field microphone positioned at the side of the test section, at a distance of 0.6 m from the cylinder model. The data were recorded with a sampling frequency of 51.2 kHz and a duration of 60 s using a 24 Bit National Instruments digital data acquisition module. In post-processing, they were transferred to the frequency domain with a Fast Fourier Transformation (FFT) on 75 % overlapping Hanning-windowed blocks of 16,384 samples. This results in a small frequency spacing of 3.125 Hz. Finally, the data were converted to power spectral densities  $L_p$  re  $20 \mu\text{Pa}$ . The experimental setup is shown in Figure 1(a) and explained in more detail in [5].

In addition to the acoustic measurements from [5], constant temperature anemometry (CTA) measurements were performed in the wake of the cylinders at a single flow speed using a Dantec single-wire P11 probe. The basic measurement setup is shown in Figure 1(b). The data were recorded with the same data acquisition module with a sampling frequency of 25.6 kHz and a duration of 80 s. Following the approach shown in [22], the probe was positioned at mid-span, one cylinder diameter downstream and one half diameter off center from the cylinders. Spectra were obtained from the recorded time signals using an FFT on 50 % overlapping blocks of 16,384 samples, yielding a frequency spacing of only 1.56 Hz. Again, the data were then converted to power spectral densities re  $1 \text{ m}^2/\text{s}$ .

The porous covered cylinders consisted of a rigid core cylinder of diameter  $d = 10 \text{ mm}$ , over which hollow cylinder disks of homogeneous, open-porous material were threaded. The resulting outer diameter



(a) Sound pressure level spectra [5] (gray line: wind tunnel background noise)  
(b) Spectra of the turbulent velocity fluctuations in the cylinder wake (small triangle indicates measurement position)

**Figure 2.** Measured spectra of the sound pressure level and of the velocity fluctuations at  $Re = 72,600$  (black line: reference cylinder, — Porous 1, — Porous 2, — Porous 3, — Porous 4, — Porous 5, — Porous 6)

$D$  is 30 mm. The length of the cylinders is 280 mm, leading to an aspect ratio of 9.3. In total, acoustic measurements were performed on twelve porous covered cylinders [5], but hot-wire measurements were only performed on a subset of six cylinders with porous cover. Those are summarized in Table 1. The present study only focuses on the latter, since the results are used for comparison with numerical results. The porous materials are characterized by their air flow resistivity  $r$ , which is a measure for the resistivity of a flow-permeable material against a fluid flow through the material.

## II.B. Results

Figure 2 shows the power spectral densities of the sound pressure, measured with the single microphone (Figure 2(a)), and those of the velocity fluctuations measured in the wake (Figure 2(b)) at a flow speed of 36.6 m/s (corresponding to a Reynolds number of  $Re = 72,600$ , based on the outer cylinder diameter  $D$ ). The main effect of the porous covers is that the spectral peak of the aeolian tone and the velocity fluctuations appears much narrower than for the reference cylinder, which is in good agreement with the results from Liu et al. [10]. Thereby, the width of the vortex shedding peak increases with increasing air flow resistivity  $r$  of the porous material. This means that materials with very low air flow resistivities result in narrower peaks and hence a reduction of the tonal noise. In addition, it is also visible that the porous covered cylinders generate less broadband noise than the non-porous reference cylinder. Again, porous materials with low air flow resistivities lead to a higher noise reduction than materials with high air flow resistivities.

It is also visible from Figure 2 that all cylinders show the vortex shedding peak at roughly the same frequency, which means that vortices are effectively only shed from the outer diameter ( $D = 0.03$  mm) of the porous covered cylinders, not from the rigid core cylinder with the diameter  $d = 10$  mm. This is even the case for porous materials with low air flow resistivities (such as the packing foam with  $r = 4,100$  Pa s/m<sup>2</sup> or Basotect with  $r = 9,800$  Pa s/m<sup>2</sup>). One possible explanation for this observation is that no sufficient amount of fluid enters the porous material and thus no vortex shedding occurs. This would most likely be due to the properties of the chosen porous materials such as their porosity and pore size, since it is known from other experimental studies that a fluid flow through porous covers is generally possible. For example, the Particle Image Velocimetry (PIV) measurements performed on perforated cylinders by Pinar et al. [23] clearly show a flow through the holes of the cylinder. Another hypothesis is that the fluid enters the cylinder and may even lead to vortex shedding at the rigid core cylinder, but that the development of vortices within the porous material is prevented. For the reference cylinder, the Strouhal number  $Sr$  associated with vortex shedding obtained from the acoustic measurements is about 0.18, while those for the porous covered cylinders are slightly higher (ranging from about 0.18 to just above 0.19). The Strouhal numbers obtained from the CTA measurements are all a little bit lower, which could be due to a slightly increased blockage of the wind tunnel

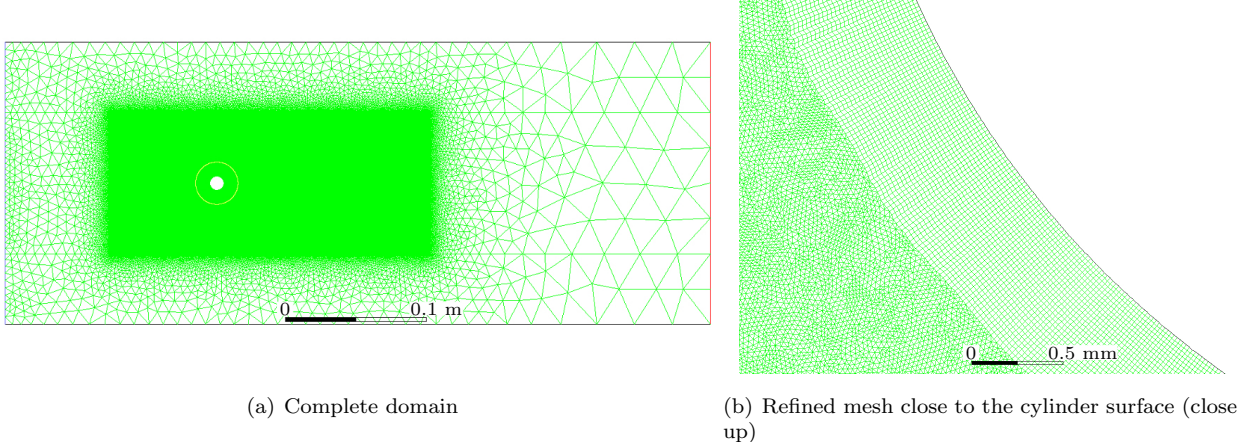


**Figure 3.** Mesh used for the numerical calculations

test section by a part of the traverse system.

Of course, the open-porous materials feature a certain surface roughness, which will also effect the flow noise generation. Past studies show that an increase of roughness will affect the flow features around the cylinder [24–27] and the noise generation. Circular cylinders with an increased roughness were found to lead to an increase of broadband noise mainly at high frequencies as well as to an increase of the vortex shedding peak and a shift of the spectra towards lower frequencies [28]. In the experimental study described here, the roughness of the porous materials was not measured. Hence, the roughness-induced effect on the noise generation cannot be clearly divided from the noise reducing effect due to the porosity.

### III. Numerical Investigation

#### III.A. Setup

The noise generated by the porous-covered cylinders was investigated numerically using a two-dimensional Detached-Eddy Simulation (DES) implemented in Ansys (Academic Version 18). It is well known that unsteady Reynolds-averaged Navier-Stokes (URANS) models are prone to fail to predict the flow physics in cases with large turbulent structures, whereas Large-Eddy Simulations (LES) require a very fine grid in the near-wall region and thus entail a high computational cost. DES is a hybrid model that functions like RANS in the near-wall regions and like LES in detached flow zones, and hence combines advantages of both methods while being less demanding than pure LES.

In the present study, the porous materials are incorporated using the *superficial velocity porous formulation*. In short, the porous media model simply adds a momentum sink in the governing momentum equations, which is done by adding a momentum source term to the standard fluid flow equations. This source term is composed of two parts, a viscous loss term and an inertial loss term. In the first term, a low velocity laminar flow through the porous medium and the resulting pressure drop across the medium are simply connected via Darcy's Law (see for example [29]), thus neglecting convective acceleration and diffusion. Basically, this corresponds to the air flow resistivity  $r$  of the materials. The second term includes inertial losses in the porous medium at high flow velocities.

In addition, the porosity  $\sigma$  (ratio of the volume of the open pores to the total volume) was set to 1 for all materials of the present study as a basic estimation. While this is a quite good approximation for any porous foams which have a porosity close to 1 (like Basotect), the porosity of the rubber granulates can be expected to be much lower. Other properties of the porous materials, like the tortuosity  $\tau$  (a measure for the twisting of the pores) or the size of the pores, are not captured. Since the DES approach employs an unsteady RANS model in the near-wall region, the effect of the porous surface on the boundary layer may not be fully reproduced. Additionally, the flow inside the medium is treated as though the solid medium has no effect on turbulence generation and dissipation. This may also lead to errors, especially if the porosity of the material and the corresponding pores are small.

The computational domain, shown in Figure 3(a), was basically chosen to resemble that of the exper-

**Table 2. Porous covered cylinders used in the numerical simulations**

Name	Note	Air Flow Resistivity( $\text{Pa s/m}^2$ )
Porous 2	similar to Basotect	9,800
Porous 4	similar to Conmetall Rubber Mat	53,200
Porous 7		1,474,300

iments. It extended 5 outer cylinder diameters  $D$  upstream of the cylinder, 10  $D$  downstream and 7  $D$  to each side of the cylinder. The boundary at the left side was set as velocity inlet and on the right side as pressure outlet, the remaining upper and lower boundaries were set as ambient walls. The mesh was refined near the cylinder wall, as shown in Figure 3(b). Thus, the dimensionless wall distance  $y^+$  takes a value of 0.54. A no-slip condition was set at the surface of the rigid core cylinder.

For appropriate temporal resolution and a maximum acoustic frequency of 5 kHz, the time step in the simulations was set to  $10^{-5}$  s and the total time was 0.22 s. This is similar to the settings used in [10]. The sound pressure was calculated for different observer positions in a distance of 0.5 m from the cylinder using the Ffowcs Williams and Hawkings (FW-H) integration method [30]. This was done for the complete simulation time. In total, calculations were performed for three different porous materials, two of which resembling cylinders used in the experiments (porous 2 and porous 4), as well as for a non-porous reference cylinder at three Reynolds numbers (based on the outer cylinder diameter  $D$ ) of 16,000, 72,600 and 106,000. The corresponding flow regime is known as the subcritical regime [31] where the boundary layer is laminar and it separates from the surface of the cylinder at about  $80^\circ$  from the forward stagnation point [22]. Table 2 gives an overview of the cylinders used in the numerical simulations.

### III.B. Results

Figure 4 shows the magnitude of the vorticity  $\vec{\omega}$  obtained for the three porous covered cylinders and the non-porous reference cylinder at Reynolds numbers of 16,000, 72,600 and 106,000. The vorticity describes the local spinning motion of the fluid particles and thus can be used to display regions of high rotational energy such as vortices.

For all cases, the periodically shed vortices are clearly visible and the vorticity increases with increasing Reynolds number. One very interesting effect that is visible from those results is that for all porous cases, fluid enters the porous covers and, consequently, vortices are also shed from the inner core cylinder. Of course, this effect is much more pronounced for cylinders with low air flow resistivities, as can be seen when comparing the plots for the cylinder with the lowest air flow resistivity (porous 2 in Figure 4(a)) with that for the cylinder with the highest air flow resistivity (porous 7 in Figure 4(g)) at the lowest Reynolds number of 16,000. Although the effect of vortex shedding from the core cylinder would be expected, it was clearly not visible in the experimental results. When the Reynolds number is increased, the amount of flow around the porous cover as well as the amount of flow through the porous material increases for all porous covered cylinders.

When comparing the results for the porous covered cylinders with those obtained for the non-porous reference cylinder, it can be seen that the wake of the porous cylinders is much slender than for the reference cylinder. This is in good agreement with results from Bruneau and Mortazavi [15], Liu et al. [10] and Naito and Fukagata [18], who state that the porous materials help to “regularize the wake”. It can also be seen that, due to the fact that for the porous covered cylinders vortex shedding also occurs at the rigid core cylinder, the vortex shedding frequency is higher and hence more vortices are visible. Thus, it can be expected that tonal noise will be generated also at a higher frequency than for the reference cylinder.

Figure 5 shows sound pressure levels obtained numerically for an observer at a distance of 0.5 m and an angle of  $90^\circ$  to the flow, which resembles the microphone position from the experiments. Although it is known that the Strouhal number associated with vortex shedding depends on the flow regime and thus on the Reynolds number (see for example [31, 32]), as a basic estimate a constant Strouhal number of 0.18 is used here to predict the frequency of the aeolian tone for means of comparison. This value for  $Sr$  corresponds to the one obtained from the acoustic experiments for the reference cylinder. It was used to predict both the frequency of the aeolian tone from vortex shedding at the outer cylinder diameter ( $D = 0.03$  m) and that from vortex shedding at the inner cylinder diameter ( $d = 0.01$ ). Both lines are included in Figure 5.

The spectra obtained at the lowest Reynolds number of 16,000 (Figure 5(a)) indicate that the tonal

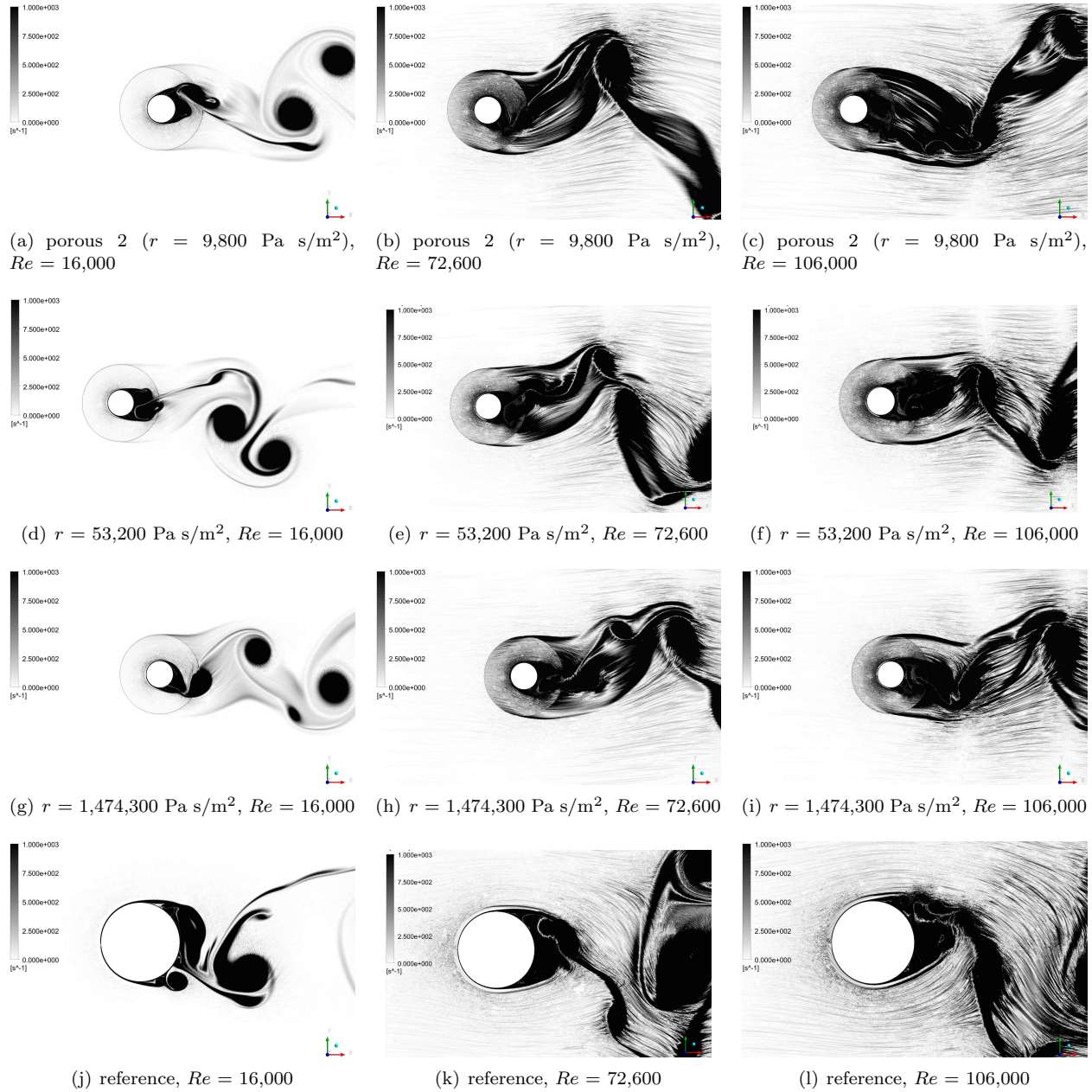


**Figure 4.** Numerically derived plots of the vorticity magnitude  $|\vec{\omega}|$  at Reynolds numbers of 16,000 (left), 72,600 (center) and 106,000 (right)

maximum for the three porous covered cylinders is due to vortex shedding at the inner core cylinder rather than the outer cylinder. Of course, the low frequency resolution may be the reason that the first peak, that should be located at a frequency below 50 Hz, is just not visible. The spectrum for the reference cylinder shows a maximum at a frequency below the estimated value, but again this may be due to the poor frequency resolution. The results for a Reynolds number of 72,600 (Figure 5(b)) show that the main peak is due to vortex shedding at the outer cylinder diameter, with a peak Strouhal number of 0.22 for the porous covered cylinders with low and medium air flow resistivity (porous 2 and porous 4) and 0.24 for the porous covered cylinder with high air flow resistivity (porous 7). In addition, the results suggest a second, much smaller spectral maximum in a frequency range that corresponds to vortex shedding at the core cylinder. The simulation results for the highest Reynolds number of 106,000, shown in Figure 5(c), show a very interesting effect: For the porous covered cylinders with low air flow resistivity (porous 2 and porous 4), the main tonal peak can be associated with vortex shedding at the outer cylinder, which is the

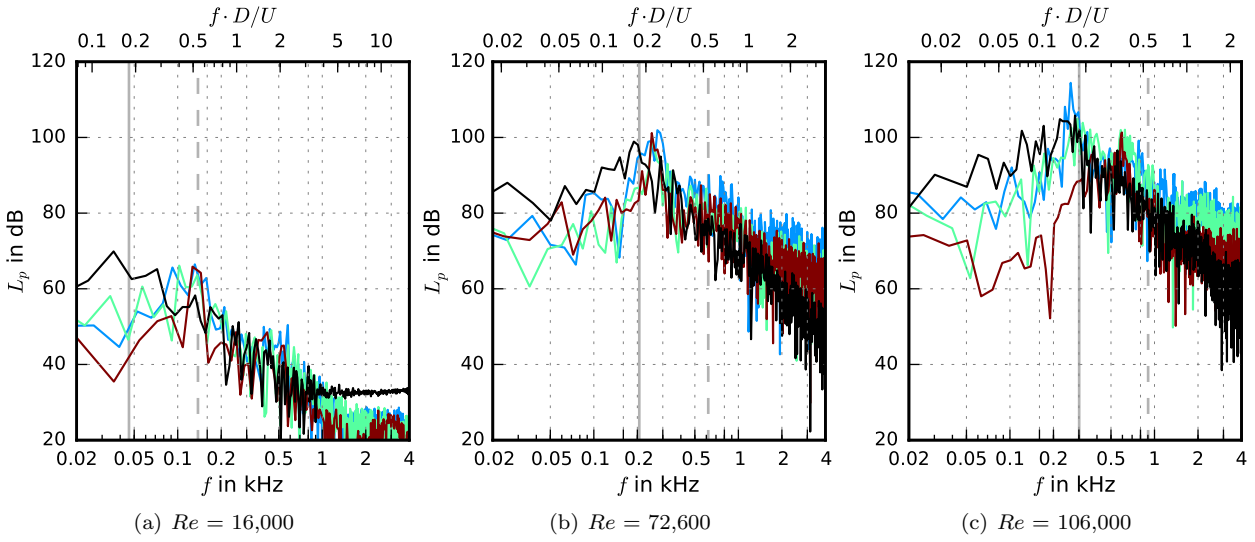


**Figure 5.** Numerically obtained sound pressure level spectra (black line: reference cylinder, blue line: Porous 2, green line: Porous 4, red line: Porous 7, gray solid line: theoretical vortex shedding frequency for  $D = 0.03$ , gray dashed line: theoretical vortex shedding frequency for  $d = 0.01$ )

same as for the reference cylinder. Additionally, a second peak can be seen at a higher frequency that is most likely due to the vortex shedding at the core cylinder. These results are pretty much expected based on the vorticity plots shown in Figure 4. However, for the porous covered cylinder with the highest air flow resistivity of  $r = 1,474,300 \text{ Pa s/m}^2$  (porous 7), no clear peak is visible that can be linked to vortex shedding at the outer cylinder diameter, although the corresponding vorticity plot (Figure 4(i)) clearly shows it. The reason for this effect is presently not clear yet. Due to the higher air flow resistivity it would be expected that less fluid is able to enter the porous material than for the other two cylinders.

In most cases shown in Figure 5, the maximum sound pressure level at the vortex shedding peak is higher for the porous covered cylinders when compared to the non-porous reference cylinder. This, however, is in agreement with the experimental results shown in Figure 2(a). As explained in [5], the effect of the examined porous covers was not to completely suppress the vortex shedding tonal noise or to minimize its amplitude, but to notably reduce the width of the tonal peak.

It is very interesting to note that the simulations predict an increase of broadband noise due to the porous covers at frequencies above the spectral peak. This clearly contradicts the results from the experiments (Figure 2(a)) and that from other studies (for example [10]). The reason for this noise increase is presently not clear. At frequencies below the aeolian tone, the simulations predict a decrease of the noise for the porous covered cylinders, which agrees with the results from the measurements.

Figure 6 shows the directivity of the vortex shedding tone at a Reynolds number of 72,600 for the reference cylinder and the three porous covered cylinders. As can be expected for cylinder flow noise, which is basically a dipole noise source, the maximum noise generation is detected at angles of  $90^\circ$  and  $270^\circ$ . It can be seen that the porous covers do not change the directivity compared to the reference cylinder. This is in agreement with the results from Liu et al. [10]. In addition, the plot again shows that the peak sound pressure level obtained for the porous covered cylinder is slightly higher in most directions than that obtained for the reference cylinder. This confirms the observations from Figure 5.

In addition to the investigation on the flow structures in the wake of the different cylinders and their flow noise generation, the simulations were also used to calculate the drag coefficient  $c_d$  of the cylinders. It is known that the resulting drag of a porous covered cylinder strongly depends on the properties of the porous material as well as on the Reynolds number. For example, Noymer et al. [12] and Naito and Fukagata [18] found a significant increase in drag at low Reynolds numbers. Liu et al. [10] observed an increase in drag only for porous covers with low porosity, whereas a porous cover with a high porosity of 0.97 lead to a notable drag reduction. A decrease of the drag coefficient with increasing permeability of the porous covers was also observed by Rashidi et al. [19]. Thereby, the porous materials can affect both the mean drag as well as the frequency and amplitude of the fluctuating drag.

Figure 7 shows the fluctuating drag coefficient  $c_d$  for the reference cylinder and the three porous covered

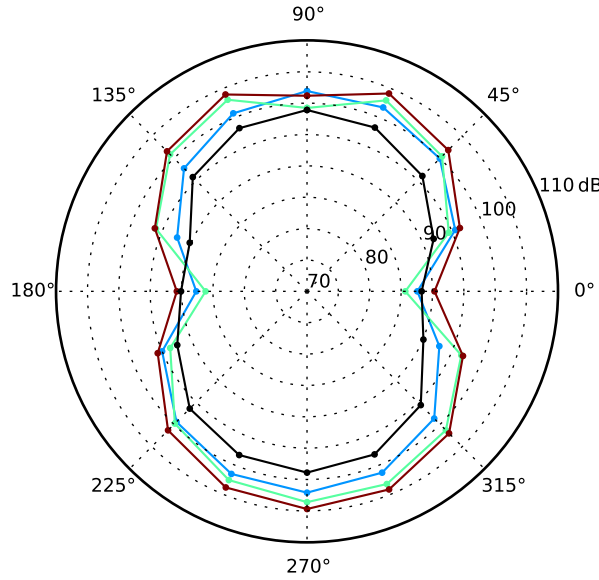


**Figure 6.** Directivity plot of the numerically obtained vortex shedding tone at  $Re = 72,600$  (flow from left to right, cylinder positioned at the center, black line: reference cylinder, — Porous 2, — Porous 4, — Porous 7)

cylinders at  $Re = 72,600$ . In addition, the time-averaged drag coefficient  $\overline{c_d}$ , averaged over the complete duration of 0.2 s, is given. In the corresponding subcritical flow regime, a mean drag coefficient of approximately 1.2 would be expected for a circular cylinder without porous cover [31, 33], whereas the simulations yield a higher value of 1.97 for the reference cylinder. However, it should be noted that it is well known that the numerical method as well as parameters like grid resolution and time step have a notable influence on the resulting drag coefficient [34]. In addition, since the drag coefficient of a circular cylinder strongly depends on the exact position where the transition to turbulence takes place in the boundary layer, DES, which employs unsteady RANS in the near-wall region, may also result in deviations.

Still, the results shown in Figure 7 show that the porous covers of the present study lead to a considerable decrease of both the amplitude of the fluctuating drag as well as the mean drag coefficient  $\overline{c_d}$ . Considering that a porosity of  $\sigma = 1$  was chosen for all three materials, this result agrees well with the results from Liu et al. [10].

#### IV. Summary and Discussion

In order to examine the aerodynamic noise generation of circular cylinders covered by porous materials, a two-dimensional Detached-Eddy Simulation was carried out. The results were compared to experimental results, which includes acoustic measurements as well as hot-wire measurements in the wake of the cylinders.

Thereby, one of the main aims of the simulations was to provide insight regarding the flow inside the porous materials. This allows to develop a better understanding of the mechanisms that are responsible for the noise reduction. Thereby, the simulations predict that fluid enters the porous cylinder covers and consequently vortices are also shed from the inner core cylinder, which was even the case for porous materials with a very high air flow resistivity. This lead to the fact that the far field noise features two tonal peaks, one associated with the outer diameter  $D$  and one with the inner diameter  $d$  of the porous covered cylinders. This effect was not observed in the experiments, which suggests that future effort has to be taken in order to improve the numerical description of the porous materials. This could be done by adding other material parameters, like tortuosity or pore size, or simply by setting a considerably lower porosity.

In the present study, it was found that the porous materials have no distinct effect on the directivity of the vortex shedding tone and that they lead to a much slenderer wake compared to the reference cylinder, which is in good agreement with several other studies. In addition, the numerical results also showed that the porous covers reduce both the amplitude of the fluctuating drag as well as the time-averaged drag coefficient.

An advantage of the simulation is that it allows an extension of the investigation towards materials with

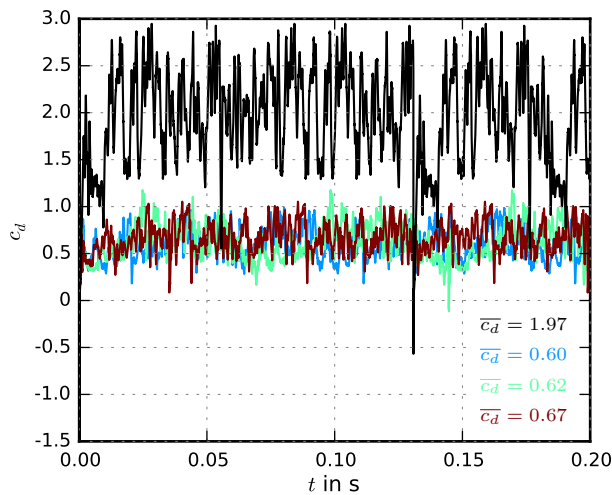


**Figure 7.** Numerically obtained drag coefficient at  $Re = 72,600$  (black line: reference cylinder, — Porous 2, — Porous 4, — Porous 7; time-averaged drag coefficient  $\bar{c}_d$  given in lower right corner)

an even lower air flow resistivity, which is not easy in the experimental investigation due to the difficulty to cut those usually very soft materials. Another advantage is that the Reynolds number can easily be extended to higher values, which is not possible with the existing aeroacoustic wind tunnel. Both approaches will be employed in future investigations.

However, the current numerical simulations also show some shortcomings, which have to be kept in mind and which, eventually, have to be overcome in future investigations. For example, certain properties of the porous materials were only approximated (such as the exact porosity) or simply neglected (such as the tortuosity or the size of the pores), although it is clear from past experiments [35] as well as from simulations by Liu et al. [10] that especially the porosity has a noticeable influence on the flow noise generation. Thus, eventually, a more realistic formulation of the porous materials will be a major target for future simulations. Furthermore, the surface roughness of the porous materials, which also has an influence on the sound pressure level spectra determined from the experiments, was not considered numerically. Finally, of course, it has to be mentioned that vortex shedding by a circular cylinder is clearly a three-dimensional phenomenon, so a two-dimensional simulation always involves some kind of simplification. However, it is worth mentioning that several well-known numerical studies, that helped to gain valuable insight on the flow around porous cylinders, were also performed on a purely 2D computational domain [10–13, 15, 16, 19].

## Acknowledgements

The authors gratefully acknowledge the funding for the work of Sparsh Sharma, which was provided by the *Graduate Research School* (GRS) of BTU within the context of a Research Assistantship, and the additional funding provided by the *Center for Flow and Transport Modelling and Measurement* (CFTM<sup>2</sup>).

## References

- <sup>1</sup>Nishimura, M., Kudo, T., Nishioka, M., Aerodynamic noise reducing techniques by using pile-fabrics. 5th AIAA/CEAS Aeroacoustics Conference, AIAA-Paper 99-1847 (1999)
- <sup>2</sup>Yahathugoda, I., Akishita, S., Experimental investigation on surface impedance effect of sound radiation from low Mach number flow around a circular cylinder. JSME International Journal Series B, 48(2), 342–349 (2005)
- <sup>3</sup>Sueki, T., Ikeda, M., Takaishi, T., Aerodynamic noise reduction using porous materials and their application to high-speed pantographs. Quarterly Report of RTRI, 50(1), 26–31 (2009)
- <sup>4</sup>Sueki, T., Takaishi, T., Ikeda, M., Arai, N., Application of porous material to reduce aerodynamic sound from bluff bodies. Fluid dynamics research, 42(1), 015004 (2010)
- <sup>5</sup>Geyer, T. F., Sarradj, E., Circular Cylinders with Soft Porous Cover for Flow Noise Reduction. Experiments in Fluids, 57(3), 1–16 (2016)
- <sup>6</sup>Showkat Ali, S. A., Liu, X., Azarpeyvand, M., Bluff Body Flow and Noise Control Using Porous Media. In 22nd AIAA/CEAS Aeroacoustics Conference, paper 2016-2754 (2016)

- <sup>7</sup>Aguiar, J., Yao, H., Liu, Y., Passive flow/noise control of a cylinder using metal foam. 23rd International Congress on Sound & Vibration (2016)
- <sup>8</sup>Yahathugoda, I., Akishita, S., Investigation on the effect of surface impedance for reducing aerodynamic sound from circular cylinder. JSME International Journal Series B Fluids and Thermal Engineering, 47(1), 67-74 (2004)
- <sup>9</sup>Suzuki, M., Sueki, T., Takaishi, T., Nakade, K., A numerical study on mechanism of aerodynamic noise reduction by porous material. The sixteenth International Congress on Sound and Vibration, ICSV 16, Kraków, Poland (2009)
- <sup>10</sup>Liu, H., Wei, J., Qu, Z., Prediction of aerodynamic noise reduction by using open-cell metal foam. Journal of Sound and Vibration, 331(7), 1483-1497 (2012)
- <sup>11</sup>Liu, H., Azarpayvand, M., Wei, J., Qu, Z. Tandem cylinder aerodynamic sound control using porous coating. Journal of Sound and Vibration, 334, 190-201 (2015)
- <sup>12</sup>Noymer, P. D., Glicksman, L. R., Devendran, A., Drag on a permeable cylinder in steady flow at moderate Reynolds numbers. Chem Eng Sci 53(16):2859-2869 (1998)
- <sup>13</sup>Bhattacharyya, S., Dhinakaran, S., Khalili, A., Fluid motion around and through a porous cylinder. Chemical Engineering Science, 61(13), 4451-4461 (2006)
- <sup>14</sup>Sobera, M. P., Kleijn, C. R., Van den Akker, H. E. A., Subcritical flow past a circular cylinder surrounded by a porous layer. Physics of fluids, 18(3) (2006)
- <sup>15</sup>Bruneau, C. H., Mortazavi, I., Numerical modelling and passive flow control using porous media. Computers & Fluids, 37(5), 488-498 (2008)
- <sup>16</sup>Zhao, M., Cheng, L. (2010). Finite element analysis of flow control using porous media. Ocean Engineering, 37(14), 1357-1366 (2010)
- <sup>17</sup>Yu, P., Zeng, Y., Lee, T. S., Chen, X. B., Low, H. T., Steady flow around and through a permeable circular cylinder. Computers & Fluids, 42(1), 1-12 (2011)
- <sup>18</sup>Naito, H., Fukagata, K. Numerical simulation of flow around a circular cylinder having porous surface. Physics of Fluids, 24(11), 117102 (2012)
- <sup>19</sup>Rashidi, S., Tamayol, A., Valipour, M. S., Shokri, N., Fluid flow and forced convection heat transfer around a solid cylinder wrapped with a porous ring. International Journal of Heat and Mass Transfer, 63, 91-100 (2013)
- <sup>20</sup>Yuan, H., Xia, C., Chen, Y., Yang, Z., Flow around a finite circular cylinder coated with porous media. 8th International Colloquium on Bluff Body Aerodynamics and Applications (2016)
- <sup>21</sup>Sarradj, E., Fritzsche, C., Geyer, T. F., Giesler, J., Acoustic and aerodynamic design and characterization of a small-scale aeroacoustic wind tunnel, Appl Acoust, 70, 1073-1080, 2009
- <sup>22</sup>Bearman, P. W., On vortex shedding from a circular cylinder in the critical Reynolds number regime, Journal of Fluid Mechanics, 37 (03), 577-585 (1969)
- <sup>23</sup>Pinar, E., Ozkan, G. M., Durhasan, T., Aksoy, M. M., Akilli, H., Sahin, B., Flow structure around perforated cylinders in shallow water. Journal of Fluids and Structures, 55, 52-63 (2015)
- <sup>24</sup>Buresti, G., The effect of surface roughness on the flow regime around circular cylinders. Journal of wind engineering and industrial Aerodynamics, 8(1-2), 105-114 (1981)
- <sup>25</sup>Kawamura, T., Kuwahara, K., Computation of high Reynolds number flow around a circular cylinder with surface roughness. In 22nd AIAA Aerospace Sciences Meeting, paper 1984-340 (1984)
- <sup>26</sup>Ribeiro, J. D., Effects of surface roughness on the two-dimensional flow past circular cylinders I: mean forces and pressures. Journal of Wind Engineering and Industrial Aerodynamics, 37(3), 299-309 (1991)
- <sup>27</sup>Ribeiro, J. D., Effects of surface roughness on the two-dimensional flow past circular cylinders II: fluctuating forces and pressures. Journal of Wind Engineering and Industrial Aerodynamics, 37(3), 311-326 (1991)
- <sup>28</sup>Alomar, A., Angland, D., Zhang, X., Molin, N., Experimental study of noise emitted by circular cylinders with large roughness. Journal of Sound and Vibration, 333(24), 6474-6497 (2014)
- <sup>29</sup>Scheidegger, A. E., The Physics of Flow through Porous Media. Third Edition, University of Toronto Press (1974)
- <sup>30</sup>Ffowcs Williams, J., Hawkings, D. L., Sound generation by turbulence and surfaces in arbitrary motion. Phil. Trans. R. Soc. Lond. A, 264(1151), 321-342 (1969)
- <sup>31</sup>Schlichting, H. Boundary-Layer Theory. Seventh Edition, McGraw-Hill Book Company New York (1979)
- <sup>32</sup>Blake, W. K., Dipole Sound from Cylinders. In *Mechanics of flow-induced sound and vibration volume 1: general concepts and elementary sources*. Academic Press Inc., London (1986)
- <sup>33</sup>Roshko, A., Experiments on the flow past a circular cylinder at very high Reynolds number. Journal of Fluid Mechanics, 10(3), 345-356 (1961)
- <sup>34</sup>Travin, A., Shur, M., Strelets, M., Spalart, P., Detached-eddy simulations past a circular cylinder. Flow, Turbulence and Combustion, 63(1-4), 293-313 (2000)
- <sup>35</sup>Geyer, T. F., Trailing Edge Noise Generation of Porous Airfoils. PhD Thesis, Brandenburg University of Technology Cottbus - Senftenberg, Cottbus, 2011